A V Chankin et al.

EDGE2D-EIRENE modelling of near SOL Er: possible impact on the H-mode power threshold

EDGE2D-EIRENE modelling of near SOL Er: possible impact on the H-mode power threshold

A.V. Chankin[a], E. Delabie[b], G. Corrigan[c], D.Harting[c], C.F. Maggi[c], H. Meyer[c]
and JET Contributors*

EUROfusion Consortium, JET, Culham Science Centre, Abingdon, OX14 3DB, UK
[a]*Max-Planck-Institut für Plasmaphysik, Garching bei München, Germany*
[b]*Oak Ridge National Laboratory,Oak Ridge, Tennessee, USA*
[c]*CCFE, Culham Science Centre, Abingdon, UK*

Abstract
Recent EDGE2D-EIRENE simulations of JET plasmas showed a significant difference between radial electric field (E_r) profiles across the separatrix in two divertor configurations, with the outer strike point on the horizontal target (HT) and vertical target (VT) [1]. Under conditions (input power, plasma density) where the HT plasma went into the H-mode, a large positive E_r spike in the near SOL was seen in the code output, leading to a very large E×B shear across the separatrix over a narrow region of a fraction of a cm width. No such E_r feature was obtained in the code solution for the VT configuration, where the H-mode power threshold was found to be twice as high as in the VT configuration. It was hypothesized that the large E×B shear across the separatrix in the HT configuration could be responsible for the turbulence suppression leading to an earlier (at lower input power) L-H transition compared to the VT configuration. In the present work these ideas are extended to cover some other experimental observations on the H-mode power threshold variation with parameters which typically are not included in the multi-machine H-mode power threshold scalings, namely: ion mass dependence (isotope H-D-T exchange), dependence on the ion ∇B drift direction, and dependence on the wall material composition (ITER-like wall versus carbon wall in JET). In all these cases EDGE2D-EIRENE modelling shows larger positive E_r spikes in the near SOL under conditions where the H-mode power threshold is lower, at least in the HT configuration.

1. Introduction

Extrapolations from present day experiments to ITER, based on the multi-machine H-mode power threshold, P_{LH}, scaling ('Martin's scaling' [2]), show that the planned auxilliary power in ITER might be marginal to trigger the L-H transition at high densities. At the same time, experimental data exhibit a factor ~ 4 scatter in P_{LH} compared to predictions of the scaling. The scaling includes a number of main operational parameters related to engineering and plasma parameters in the plasma core, but leaves out even larger number of unaccounted parameters describing particularities of experimental conditions.

It has been observed since the discovery of the H-mode in ASDEX that wall conditions, magnetic equilibrium, geometry of the divertor (e.g. open or closed for neutrals), methods of density control and some other factors have a large impact on the ability to initiate the L-H

transition at a given input power, P_{input} [3,4]. They are not covered by the P_{LH} scaling, but can explain the scatter of experimental P_{LH}. Most of these factors describe conditions in the extreme edge of the plasma (encompassing SOL, divertor and a narrow layer around the separatrix).

One of the most widely observed signatures of the divertor geometry's influence on the P_{LH} is the effect of the X-point height, where lowering the distance between the X-point and the divertor target (or the 'dome', separating inner and outer halves of the divertor) led to the reduction in P_{LH} in JET[5,6], MAST[7], DIII-D [8]. Lowering the X-point height involves the reduction of the 'outer leg length' (the poloidal distance between the X-point and the outer strike point (OSP) within the flux surface) and sometimes the shift of the OSP from the vertical to the horizontal target (see e.g. results from Alcator C-Mod [9] where all three effects were present), making interpretation of experimental results more difficult. In recent experiments in JET a

factor two reduction of P_{LH} was observed when the OSP position was shifted from the vertical target (VT) to the horizontal target (HT) [10-12] (the X-point height however was also reduced, as well as the 'inner leg length'). The magnetic equilibria in the divertor are shown in Fig. 1.

The JET experiments [10-12] initiated EDGE2D-EIRENE code simulations with drifts and parallel currents aimed at understanding mechanism(s) behind the influence of the divertor configuration (HT or VT configuration) on P_{LH} (see the mechanism description in [12], with more details in [1]). The simulations revealed a significant difference between radial electric field (E_r) profiles across the separatrix in

Fig. 1. Magnetic configurations of the HT (#81883) and VT (#84727) JET pulses in the divertor.

the two configurations. At the P_{input} close to that where the HT pulse went into the H-mode the E_r showed a large positive spike in the near SOL, apparently caused by the target T_e spike. Since the E_r was negative in the core (no external toroidal momentum input was assumed in the code runs), the positive E_r spike in the near SOL implied a very large E×B shear across the separatrix over a narrow region of a fraction of a cm width. In the VT configuration no such E_r spike was seen in the near SOL and the E×B shear was much lower. It was hypothesized that the large E×B shear around the separatrix position in the HT configuration could facilitate earlier (at lower P_{input}) edge turbulence suppression and hence lower P_{LH} in this configuration.

The origin of the target T_e spike at a strike point in the HT configuration and its absence in the VT configuration for comparable P_{input} levels was explained by the difference in the ionization pattern of neutrals recycling near the OSP. Simulations suggest that the low Te at the near-SOL target is due to strong ionization in that region. Traditionally, this strong ionization has been attributed to the direct recycling of neutrals into the near SOL [13]. However, recent simulation analysis has shown that on JET the near SOL ionization results from more complicated indirect neutral pathways. Neutrals recycling from both inner and outer targets, reflecting from the lower tiles, crossing the PFR and ionizing in the near SOL are actually responsible for the majority of ionization in the near SOL, low T_e region, and these effects are stronger in VT configurations
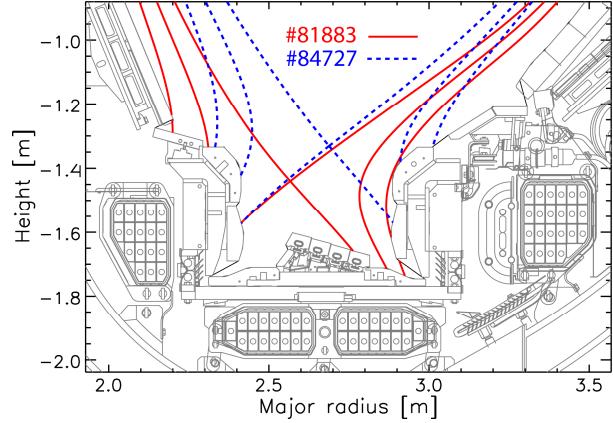
[14]. As a result, in VT configurations low T_e and high n_e plasma at the OSP is formed. The outer target (OT) T_e rises radially over short distances corresponding to the near SOL when mapped to the flux surfaces. In contrast, in HT configurations n_e near the OSP is low and target T_e tends to peak there, decaying across the target outward (towards the wall). The difference in the OT T_e profiles between the two configurations, via the mechanisms of Debye sheath drop at the target ($\sim 3T_e/e$) and contributions to the parallel electron momentum balance by $\nabla_\parallel p_e$ and $\nabla_\parallel T_e$ terms, leads to the difference in the SOL E_r profiles described above ([12,1]).

In the present work these ideas are extended to cover some other experimental observations on the P_{LH} variation with parameters which typically are not included in the multi-machine P_{LH} scalings, namely: ion mass dependence (isotope H-D-T exchange), dependence on the ion ∇B direction, and dependence on the wall material composition (ITER-like wall versus carbon wall in JET). In all these cases EDGE2D-EIRENE modelling shows larger positive E_r spikes in the near SOL under conditions where the P_{LH} is lower, at least in the HT configuration.

2. Setup of EDGE2D-EIRENE cases

EDGE2D-EIRENE grids were built using magnetic equilibria of JET pulses #81883 and #84727, for which equilibria in the divertor are shown in Fig. 1. In the radial direction, each grid has 12 poloidal rings in the core, 20 in the SOL and 8 in the private flux region (PFR). In the poloidal direction, each grid has 52 rows in the core and 20 rows in each inner and outer divertor, hence, 92 rows in the SOL and divertor. The grids were optimized for numerical stability of the code
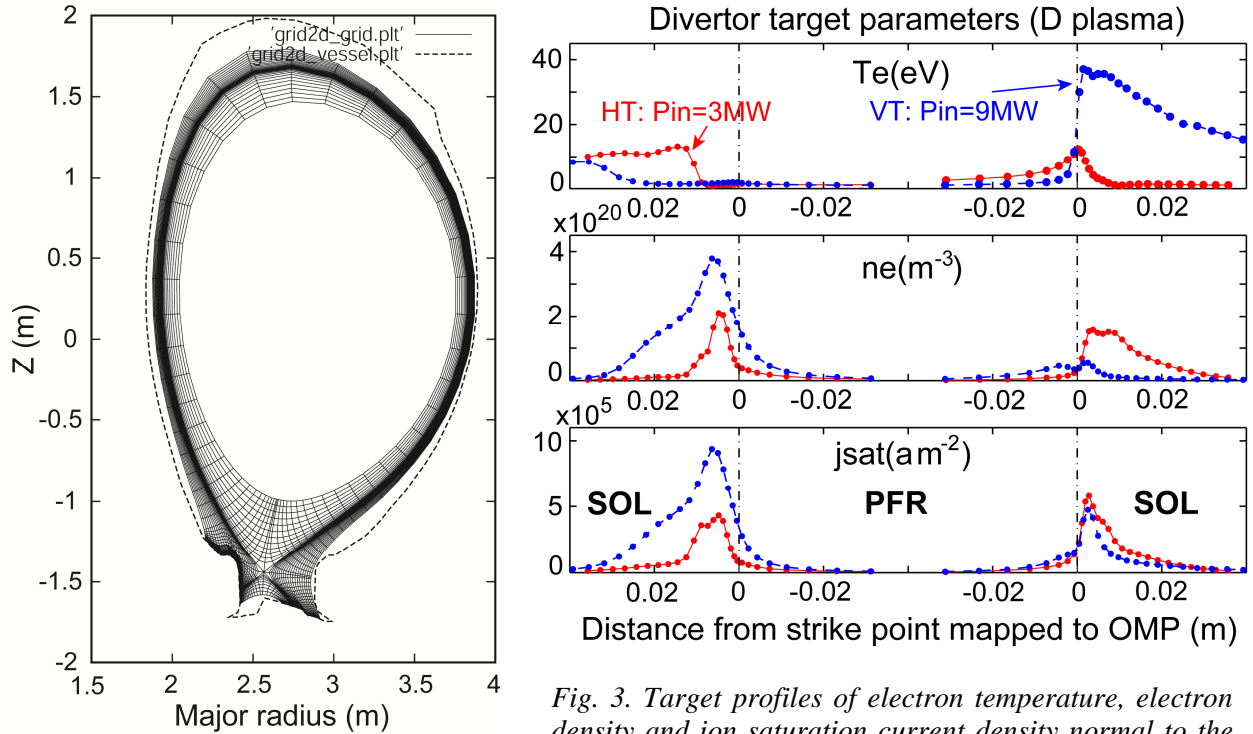

Fig. 2. The grid used for EDGE2D-EIRENE modelling (example of the JET HT configuration of #81883 is shown).

Fig. 3. Target profiles of electron temperature, electron density and ion saturation current density normal to the targets in the two EDGE2D-EIRENE cases which were chosen as a basis for other scans/studies in this work.

3

runs in the presence of drifts and parallel currents which were switched on across the entire computational domain. For most of the code runs, material surfaces were assumed as in the ITER-like Wall (ILW), except for a few runs where carbon wall ('C wall') in which JET operated earlier was assumed. Only pure deuterium (D), or its isotopes: hydrogen (H) or tritium (T), plasmas were modelled. Earlier simulations with the inclusion of beryllium sputtered from the ILW showed only its minor influence on the code results due to its small radiated power in the divertor. Another motivation for modelling only pure H isotope plasmas was to facilitate analysis of the code output by isolating effects of main ion neutrals' mobility from those of impurity radiation. Tungsten was also not included in the ion mixture, as its concentrations inside of the plasma covered by the EDGE2D-EIRENE grid were found to be negligible.

A self-consistent neoclassical model for E_r was implemented in the core which impeded surface averaged radial currents.

The EIRENE version with Kotov-2008 model was used to describe neutral behaviour. The plasma density was controlled by a combination of gas puff from the PFR and wall recycling ('puff + recycling' option in EDGE2D-EIRENE), aiming at maintaining a specified electron density at the outer midplane (OMP) position of the separatrix, $n_{e,sep}$, which was kept at 1.2e19 m^{-3} in all cases. Spatially constant anomalous transport coefficients were specified for all cases: $D_\perp=1$ m^{2}s^{-1} and $\chi_{e,i}=2$ m^{2}s^{-1} across the whole grid.

The P_{input} into the grid was set at 3.0 MW in the HT case, which is close to the experimental value for the P_{LH} in this configuration. A much higher P_{input}, 9.0 MW, had to be used in the VT case in order to achieve (marginally) peaked OT T_e. At lower P_{input}, the OT T_e profile had a maximum outside of the OSP. At the same time, in the experiment the VT plasma required only a factor of two higher P_{input}, rather than factor 3, for the L-H transition compared to the HT plasma. Target profiles for the two pure D cases which were chosen as a base for other scans in this study are shown in Fig. 3. In all cases described here, the P_{input} into the grid was equally split between ion and electron channels.

3. H-D-T scans in HT configuration
The most-clear cut trends were obtained in the HT configuration described in this section, while in the VT configuration it was difficult to obtain code solutions with peaked T_e profiles at the OSP, as mentioned earlier. The code results in the VT configuration will be discussed in section 6.

In the isotope exchange experiments in JET, P_{LH} was found to be the highest in the H plasma, lower in the D plasma and the lowest in the pure T plasma. P_{LH} in mixed isotope plasmas was found to be in between pulses with pure isotope plasmas. A nearly inverse scaling of the power crossing the separatrix just before the L-H transition against the average mass of an H isotope was established in the experiments [15]. It is therefore of interest to check whether the amplitude of the positive E_r spike seen in the near SOL in EDGE2D-EIRENE H-D-T scan cases correlates with the experimentally observed P_{LH}: an increase in the amplitude of the E_r spike with the increase in the mass of the H isotope may indicate a possible causality between the E_r spike and, hence, the E×B shear across the separatrix, and earlier (at lower P_{input}) onset of the L-H transition.

Target T_e profiles mapped to the OMP and E_r profiles at the OMP for the H-D-T scan are shown in Fig. 4. All input parameters in EDGE2D-EIRENE cases were the same except for the varying H isotope. The OT T_e spike is highest in the T case, resulting in the highest near SOL E_r spike and the highest E×B shear. The reason for the highest T_e spike in the T case is the lowest mobility of T neutrals due to their highest mass. In EDGE2D-EIRENE cases that reached the steady state (and only such cases are considered in this work) the net ion flux outward, through each closed flux surface into the SOL, is equal to the neutrals flux inward. Hence, the outward plasma (ion) flux Γ_i and the plasma convective energy flux $5/2\Gamma_i(T_e + T_i)$ are lowest in the T case. Since the P_{input} into the grid is the same for all cases, the conductive energy flux $n\chi_e\nabla T_e + n\chi_i\nabla T_i$ must be the highest in the T case, resulting in the highest $T_{e,i}$ across the grid, and, in particular, highest $T_{e,i}$ at the separatrix, which, in turn, give highest power flux to the target and highest target $T_{e,i}$. In the code output ion fluxes through the separatrix are: 2.02×10^{22}, 1.31×10^{22} and 1.10×10^{22} s^{-1} leading to highest separatrix T_e and T_i in T cases, see Table 1. This table also gives code results for ion fluxes through the separatrix, radiated power P_{rad} (only on hydrogen isotopes, since there are no impurities in the modelling), the fraction of P_{rad} from the core part of the computational grid in the total P_{rad}, and separatrix T_e and T_i at OMP, for the cases considered in this section as well as for some other cases discussed later in sections 5 and 6.
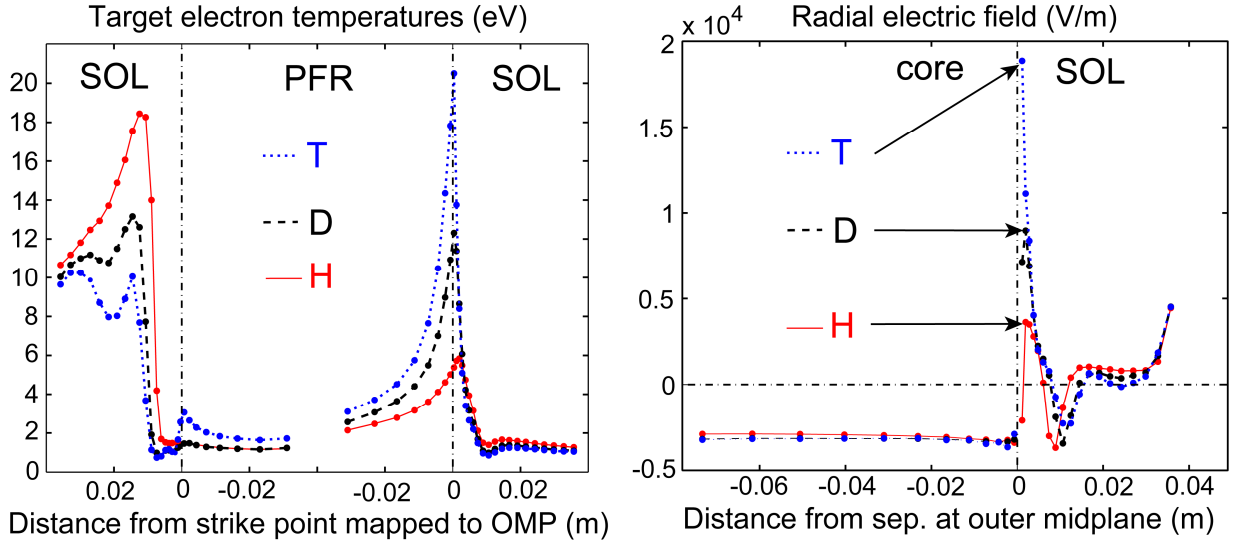

Fig. 4. Target T_e profiles (left) and radial electric field profiles (right) in EDGE2D-EIRENE cases in the HT configuration in pure H, D and T plasmas.

The inner target plasma parameters should have a very small contribution to the near SOL E_r due to very low T_e's around the inner strike point. The OMP T_e difference between H and T cases, only 3.2 eV (5.8%), may seem insignificant and not being able to explain a large, factor 3.51 difference in peak OT T_e values between T and H cases. A number of mechanisms however contribute towards the increase in the difference between peak target T_e's. The first mechanism follows from the two point model which relates upstream (OMP in this case) and downstream (target) T_e. Owing to the strong dependence of the parallel electron heat flux on the upstream T_e: $q_{e\parallel} \propto T_{e,u}^{7/2}$, following from the two point model for the case of a large T_e drop to the target

5

(which is the case here), the difference in separatrix OMP T_e's between the two cases translates into a factor ~ 1.22 difference in $q_{e\parallel}$.

Parameter→ ↓case	Ion flux thr. sep. (s^{-1})	T_e (eV) at OMP	T_i (eV) at OMP	P_{rad} (MW)	Core P_{rad} frac. (%)
H	2.02E22	54.9	65.4	4.59E-01	5.68
D	1.31E22	57.4	70.4	4.75E-01	3.59
T	1.10E22	58.1	86.0	4.61E-01	3.08
H_Rev.Bt	2.32E22	54.1	69.0	3.93E-01	7.66
D_Rev.Bt	1.62E22	57.1	75.1	3.83E-01	5.56
T_Rev.Bt	1.33E22	58.3	86.2	3.75E-01	4.73
D (C wall)	1.23E22	58.0	81.7	4.70E-01	3.34

Table 1. Ion fluxes through the separatrix, radiated power P_{rad}, the fraction of P_{rad} from the core part of the computational grid, separatrix T_e and T_i at OMP, for the H-D-T series of cases; the same for reversed B_t cases and for a D case in the carbon (C) wall environment .

Neglecting radiation losses, the electron heat flux to the target should scale as $q_{e\parallel} = q_{e,t} \propto n_{e,t} T_{e,t}^{3/2}$. As pressure tends to reach equilibrium along field lines, one can add here an equation $n_{e,t} T_{e,t} \propto n_{e,u} T_{e,u}$ (and here we ignore the difference between T_e and T_i for simplicity). Combining above three equations yields the scaling: $T_{e,t} \propto T_{e,u}^5 / n_{e,u}^2$. Since the upstream plasma density $n_{e,u}$ was the same in all cases, the small, 5.8% difference in OMP T_e's translates into a much greater, factor 1.33 difference in target T_e's.

The second mechanism is a positive feedback loop that exists between falling $T_{e,t}$, rising $n_{e,t}$ (due to the pressure tendency to be constant along field lines) and rising radiation in the divertor $\sim n_{e,u}^2$ (unless $T_{e,t}$ is extremely low so that the plasma is detached from the target, which is not the case here). The influence of this factor is difficult to quantify, but it may be significant, since hydrogen (or its isotopes) radiation is playing a certain role in the cases analyzed ($\approx$15% of P_{input}, as follows from Table 1).

Finally, the separatrix OMP T_i difference between H and T cases, factor 1.31, is much greater than the 5.8% OMP T_e difference, which should contribute to a difference in the total parallel power flux into the divertor via (mostly) the ion heat convection channel.

Different neutral penetration and ionization in the plasma in the H-D-T series of cases impacts radial profiles of plasma parameters shown in Fig. 5. The density profile shows the largest rise across the SOL and the core in the H case. This, given the same power input for all three cases, results in opposite trends for T_e and T_i profiles, which are the flattest in the H case. Since power flux to the target is mostly due to electron parallel heat conduction which scales as $T_{e,u}^{7/2}$, upstream T_e profiles in the SOL are the least affected by the isotope exchange. Overall, changes in the profiles are quite modest, which agrees with small variation of the E_r profiles in the core seen in Fig. 4. The total radiation power is similar in all three cases, and the fraction of P_{rad} radiated in the core is small, see Table 1. Among all parameters analysed, it is the ion flux through the separatrix which shows the largest variation between H, D and T cases, confirming that it is primarily responsible of the target T_e and upstream E_r variation.
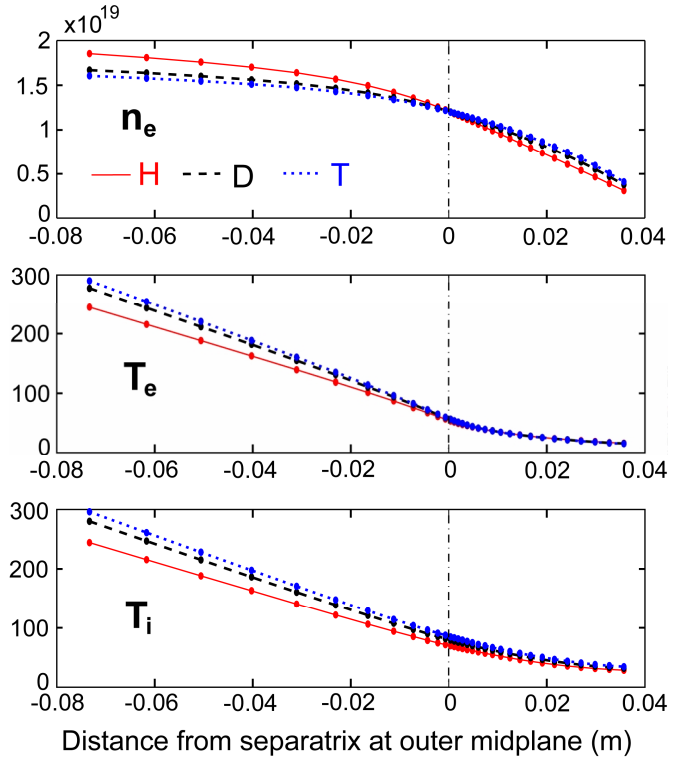

Fig.5. OMP profiles of plasma parameters for the H-D-T series of cases.

4. Normal/forward vs. reversed B_t cases (HT configuration)

It is well known, since early experiments with the H-mode in ASDEX [3], that in single X-point divertor configurations access to the H-mode strongly depends on the toroidal field direction: in the configuration with the ion ∇B drift directed towards the X-point ('normal', or 'forward' B_t direction) P_{LH} is by factor two lower than when it is directed away from the X-point ('reversed' B_t direction). Shortly after these experimental observations were made on ASDEX, neoclassical effects (related to classical drifts) which take into account the existence of the X-point and SOL were invoked to explain the experiment [16,17]. It is however also of interest to check whether an alternative explanation for the effect of the ion ∇B drift direction, related to changes in the near SOL E_r, is possible. As one can see by comparing E_r profiles shown in Figs. 4 and 6 for normal and reversed B_t configurations, respectively, E_r is larger in the normal B_t configuration. In order to obtain solutions shown in Fig. 6, directions of all drifts were reversed in EDGE2D.

Toroidal field reversal in known to influence target asymmetries (see e.g. [18]). In reversed B_t cases (Fig. 6), owing to lower and less peaked T_e at OT (the exception to this however may be the case in hydrogen) and rising IT T_e across the inner strike point, in the direction from the PFR to the SOL (which should make a negative contribution, $E_r < 0$, to the E_r at the OMP) the E_r spikes at the OMP are smaller that those in the cases in the normal B_t configuration (Fig. 4). This indicates the smaller E×B shear across the separatrix than in the normal B_t configuration, potentially leading to a later (at higher P_{input}) L-H transition.
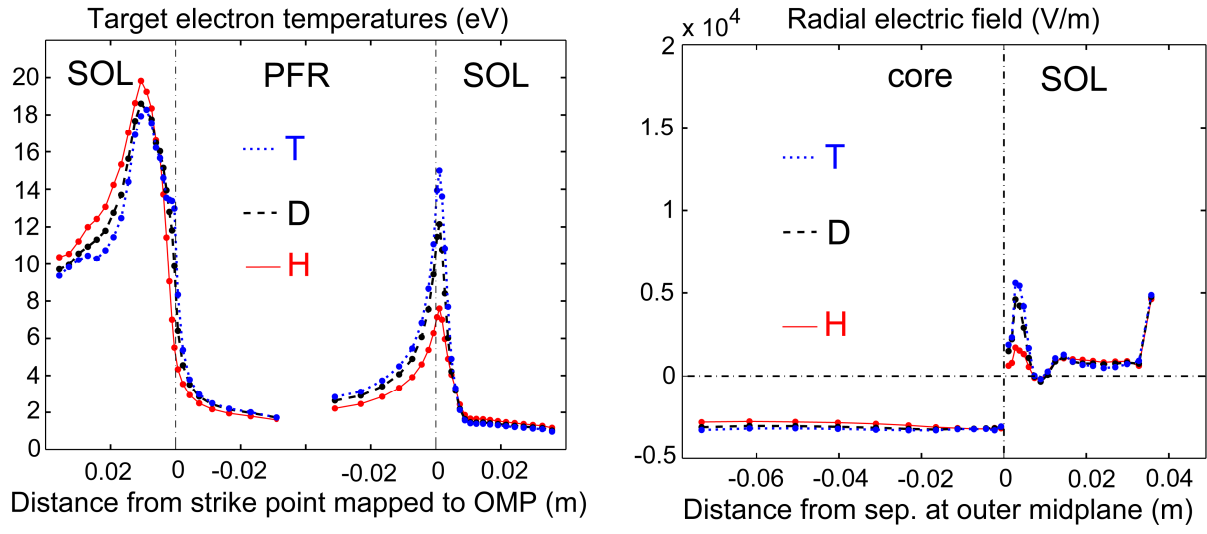
Fig. 6. Target T_e (left) and radial electric field at OMP (right) profiles in EDGE2D-EIRENE cases in the HT configuration in pure H, D and T plasmas, in the reversed B_t configuration.

OMP n_e, T_e and T_i profiles for the cases in reversed B_t are almost identical to those in the normal B_t, shown in Fig. 4. From parameters shown in Table 1, one can see trends towards lower total P_{rad} and higher core P_{rad} fractions in reversed B_t cases. The values, and their changes associated with the field reversal, however, are fairly low, and are unlikely to make a significant impact on changes in separatrix T_e and T_i at OMP. This leaves changes in divertor/target asymmetries associated with the field reversal the prime candidate to explain lower SOL E_r in reversed B_t configurations.

5. ITER-like Wall (ILW) vs carbon wall (HT configuration)

In JET experiments in ILW, in the high density branch the P_{LH} was found to be reduced by ~ 30%, and by ~40% when the radiation from the bulk plasma is subtracted, giving power across the separatrix, P_{sep}, compared to the P_{LH} in carbon wall plasmas, for the same engineering and plasma parameters, in particular, the same line average density [11]. Lower P_{LH}, by 25%, was also found in ASDEX Upgrade in the full tungsten (W) wall compared to earlier discharges in the mixed graphite (C) and W environment, despite higher edge density, higher gas puff and stronger degree of detachment in the full W discharge [19]. The lower P_{LH} in the W wall was found to correlate with higher edge density as well as steeper edge density gradient. The calculated minimum in the neoclassical E_r inside the separatrix was found to be the same for both wall materials before the L-H transition [19]. In JET experiments, however, no significant differences were observed between core density profiles in comparable discharges in C and ILW. From the EDGE2D-EIRENE modelling described here, with fixed $n_{e,sep}$ no significant differences between the two D cases can be seen in Table 1, except for somewhat higher OMP separatrix T_i in the carbon environment case. OMP n_e, T_e and T_i profiles in the C environment cases are also nearly identical to those in the ILW case shown in Fig. 4 (for the D case).

Figure 7 shows target T_e (left) and E_r at OMP (right) profiles in EDGE2D-EIRENE cases in the HT configuration in pure D plasmas in ILW and C wall. The ILW case is the same as the D case plotted in Fig. 4. For the C wall case exactly the same settings were used as for the ILW case,

only the wall material was changed to carbon, which influenced plasma-surface interactions (see below). Larger peak T_e's can be seen at both targets in the ILW case, which is translated into larger E_r spikes, which is, qualitatively, in line with experimental observations of lower P_{LH} in ILW.
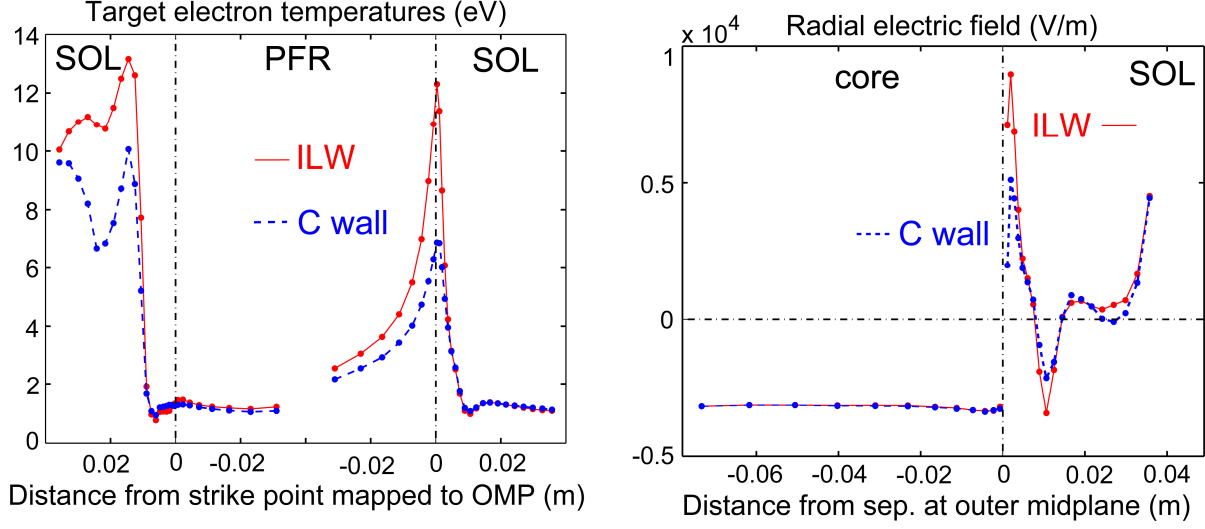

Fig. 7. Target T_e (left) and radial electric field profiles at OMP (right) in EDGE2D-EIRENE cases in the HT configuration in pure D plasmas in the ILW and carbon wall (C wall) environments.

Since deuterium was the only ion species present in these cases, there was no physical or chemical sputtering of carbon. In the experiment one can only consider an almost pure D case (ignoring a small fraction of W ions) in the ILW, provided there is no external impurity source (e.g. N or Ne puffing). In the C wall environment, on the other hand, carbon, being an intrinsic impurity, is produced by both physical and chemical sputtering, so the real plasma always has some C impurity content. If one was to include an inevitable C radiation in the EDGE2D-EIRENE case, target T_e's would drop stronger resulting in even smaller E_r spikes. Hence, the comparison between the two cases considered here provides a lower estimate for differences in the T_e and E_r profiles, and in a real situation these differences can be even stronger. Unfortunately, cases with drifts and carbon impurities for main plasma parameters specified in this work could not be run due to numerical instabilities.

As pointed out above, the ILW and C wall cases only had one difference in EDGE2D-EIRENE settings: the material of the walls. Since most of neutral recycling takes place in the divertor, the heavier W surface there is expected to reflect more neutral (mostly D atom's) kinetic energy back to the plasma (or, to absorb less energy) than the lighter C surface. To estimate the influence of the neutral-wall interaction on the difference in energy balance between the two walls, calculations were carried out where the plasma and neutral background from the C wall case were taken as an input to the Monte Carlo neutral code EIRENE, which was then run for one step in both C wall and ILW environments. EIRENE returns, among many other parameters, energy reflected from the wall by circulating neutrals. It was found that in the C wall case, 0.247 MW of energy was returned back to the plasma from the wall, compared to 0.555 MW when the C wall is replaced with the ILW. The difference, ≈ 0.3 MW, represents $\approx 10\%$ of the total P_{input} (3 MW). These 10% of input power may be considered as an extra input power into the plasma,

9

from the divertor side, by ILW compared to the C wall, which can explain higher target T_e's in ILW. In these EIRENE calculations it was found that the main chamber wall contribution to the plasma energy balance was opposite to that of the divertor, in agreement with the expected lower energy reflecting coefficients from beryllium (which is part of the ILW) compared to carbon. The contribution of the main chamber recycling to the overall recycling in the EDGE2D-EIRENE cases was however insignificant, so the plasma energy balance was mostly affected by the neutral recycling in the divertor.

6. EDGE2D-EIRENE results in the VT configuration

As was already pointed out in Sec. 2, a much higher P_{input} into the EDGE2D-EIRENE computational grid, up to 9 MW, had to be specified in order to achieve even marginally peaked T_e profile at the OT in the reference pure D case (see Fig. 3), whereas in the experiment the P_{LH} is approximately only factor 2 higher than in the HT configuration. It is possible to reduce the P_{input} necessary to obtain peaked OT T_e profiles near the strike point in the EDGE2D-EIRENE modelling by choosing lower transport coefficients near the separatrix. This, however, would necessitate also using lower transport coefficients in the HT cases, which would adversely impact the consistency between the code and experimental target profiles. The other option would be to assume different transport coefficients in cases in HT and VT configurations. This would however introduce arbitrary elements in the code modelling, and there are no sufficient physics reasons to assume lower transport coefficients in VT cases, which would facilitate peaking of T_e profiles near OT. At the same time, in the experiment there seems to be no evidence for strongly peaked target T_e profiles in VT configurations near the H-mode power threshold. Therefore, there are presently no strong reasons to believe that near SOL E_r spikes play important role in the L-H transition in VT configurations.
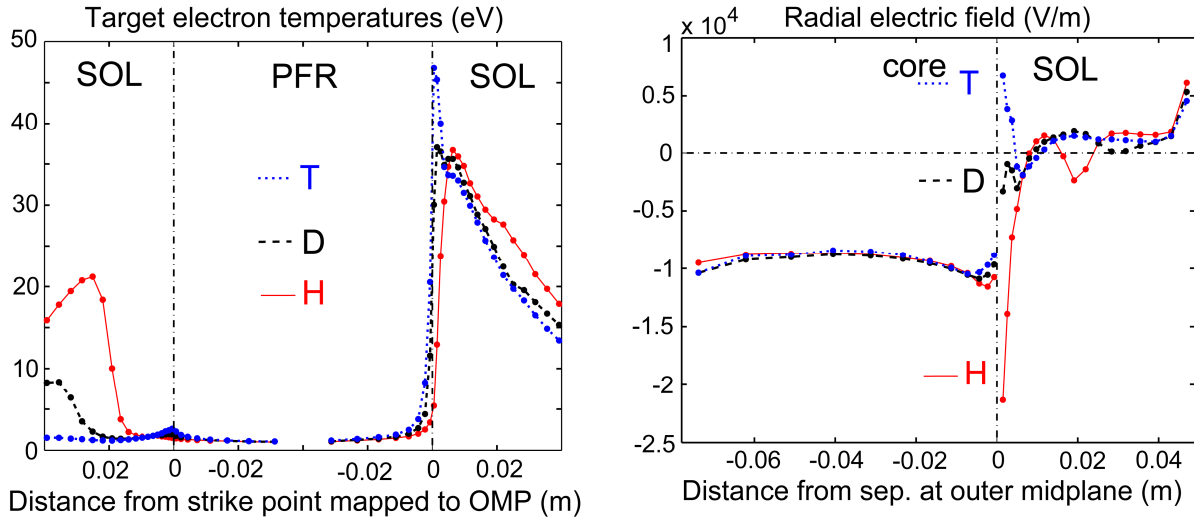

Fig. 8. The same profiles as potted in Fig. 4, but for cases in the VT configuration with 9 MW of the input power.

In the EDGE2D-EIRENE modelling, basically the same trends can be seen as in the HT configuration, except for the case in hydrogen (H) which clearly falls out of the trend by not showing a peaked T_e profile at the OT. To achieve such a peaking, an even higher P_{input} would be

necessary. As an example, Figure 8 shows the same profiles as those plotted in Fig. 4, but for the cases in the VT configuration with 9 MW of P_{input}.

7. Summary

Recent JET results on the influence of divertor geometry on H-mode power threshold and their explanation via target T_e profiles and the E×B shear in the near SOL triggered explorative EDGE2D-EIRENE modelling. A number of dedicated code cases aimed at establishing correlations between experimental results on the effect of isotope (H-D-T) exchange, toroidal field reversal and replacement of carbon with the ITER-like wall on the P_{LH}, on the one side, and near SOL E_r shear in code solutions, on the other side, was run. In the JET horizontal (outer) target (HT) configuration, amplitudes of near SOL E_r spikes in EDGE2D-EIRENE solutions do indeed anti-correlate with experimental observations of P_{LH}.

Given narrowness of E_r spikes in the code solutions (a fraction of a cm), the correlations obtained prompt a theoretical study on whether such narrow E×B shear layers can lead to edge turbulence suppression and therefore causality between near SOL E_r spikes and the L-H transition, the issue not addressed in this work.

Contrary to results obtained in the HT configuration, E_r spikes in the near SOL are difficult to obtain in the JET vertical (outer) target (VT) configuration. Code modelling with the same assumptions for separatrix electron density and anomalous transport coefficients require at least factor 3 increase in the input power (P_{input}) in the computational domain in order to obtain similar E_r profiles as in the HT configuration. At the same time, in the experiment it requires only a factor 2 increase in P_{input} to trigger the L-H transition, compared to the P_{input} level where the L-H transition was observed in the HT configuration. This indicates that near SOL arguments may not apply (or, at least, not fully apply) to VT configurations.

11

References

[1] Chankin A V et al., Possible influence of near SOL plasma on the H-mode power threshold, Nuclear Materials and Energy (2016), http://dx.doi.org/10.1016/j.nme.2016.10.004

[2] Martin Y R, Takizuka T and ITPA CDBM H-mode Threshold Database Working Group, 2008 J. Physics **123** 012033

[3] Wagner F, Bartiromo R, Becker G *et al* 1985 **25** 1490

[4] Bosch H-S, Fuchs J C, Gafert J *et al* 1999 Plasma Phys. Control. Fusion 41 A401-A408

[5] Horton L D 2000 Plasma Phys. Control Fusion **42** A37-A49

[6] Andrew Y, Hawkes N C, O'Mullane M G *et al* 2004 Plasma Phys. Control Fusion **46** A87-A93

[7] Meyer H, De Bock M F M., Conway N J *et al* 2011 Nucl. Fusion **51** 113011

[8] Gohil P, Evans T E, Fenstermacher M E *et al* 2011 Nucl. Fusion **51** 103029

[9] Ma Y, Hughes J W, Hubbard A E, LaBombard B and Terry J 2012 Plasma Phys. Control. Fusion **54** 082002

[10] Meyer H, Delabie E, Maggi C F *et al* 2014 41st EPS Conf. on Plasma Phys., 23-27 June 2014, Berlin, Germany, paper P1.013, http://ocs.ciemat.es/EPS2014PAP/pdf/P1.013.pdf

[11] Maggi C, Delabie E, Biewer T M *et al* 2014 Nucl. Fusion **54** 023007

[12] Delabie E, Chankin A V, Maggi C F *et al* 2015 42nd EPS Conf. on Plasma Phys., 22-26 June 2015 Lisbon, Portugal, paper O3.113, http://ocs.ciemat.es/EPS2015PAP/pdf/O3.113.pdf

[13] Loarte A 2001 Plasma Phys. Control. Fusion **43** R183-R244

[14] Moulton D, private communication.

[15] Righi E, Bartlett D V, Christiansen J P *et al* 1999 Nucl. Fusion **39** 309

[16] Hinton F L 1985 Nucl. Fusion **25** 1457

[17] Hinton F L, Staebler G M 1989 Nucl. Fusion **29** 405

[18] Chankin A V 1997 J. Nucl. Mater. **241-243** 199

[19] Shao L N, Wolfrum E, Ryter F *et al* 2016 Plasma Phys. Control. Fusion **58** 025004